3D-ID

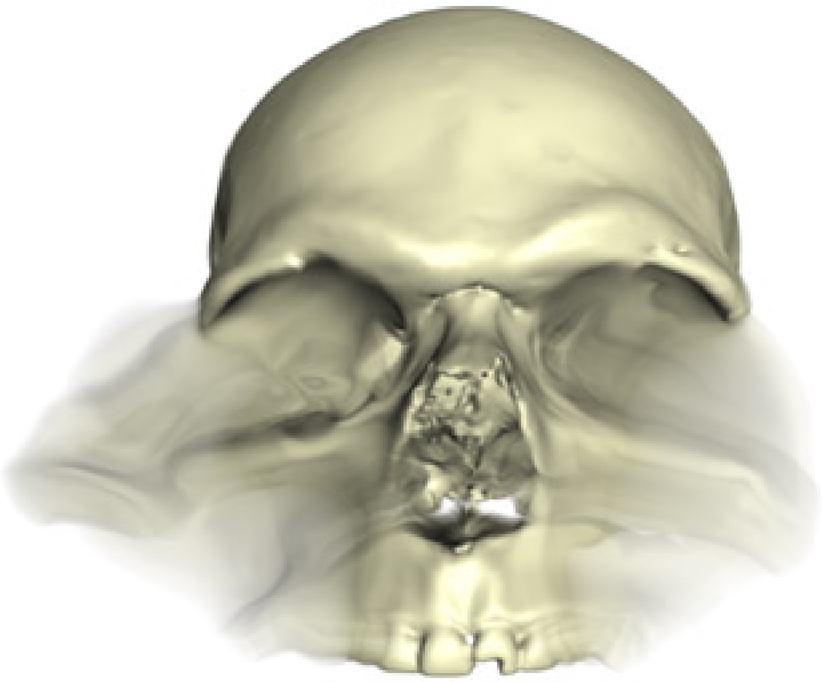

Geometric Morphometric Classification of Crania for Forensic Scientists

Dennis E. Slice and Ann Ross

Sponsored in part by
National Institute of Justice Grant
2005-MU-BX-K078
to
Ann Ross

VERSION: 1.0 (16JAN2010)

CREDITS:

FORENSIC ANTHROPOLOGY

Ann Ross
North Carolina State University
Raleigh, North Carolina, USA

PROGRAMMING AND STATISTICS

Dennis E. Slice
Florida State University
Tallahassee, Florida, USA

COVER/SPLASH IMAGE

Rob O'Neill
Pratt Institute
http://www.morphometric.com/

ACKNOWLEDGEMENTS: The authors wish to thank the following for their assistance and cooperation in various ways: Eugenio Aspillaga (Universidad de Chile), Greg Berg, Hugo Cardoso (Bocage Museum, Portugal), María Dolores Garralda (Universidad Complutense, Spain), Richard Jantz, Erin Kimmerle, Antonio Martinez, Janet Monge, Jose Vicente Pachar (Director General, Instituto de Medicina Legal y Ciencias Forenses, Panama), Juan Carlos Prados (Departamento de Anatomía e Embrología Humana, Spain), José Luis Prieto (Instituto Anatómico Forense, Spain), Rick Snow, Kate Spradley, Doug Ubelaker, Danny Wescott, Shanna Williams, American Museum of Natural History, C.A. Pound Human Identification Lab, Georgia Bureau of Investigation, North Carolina Office of the Chief Medical Examiner.

END-USER LICENSE AGREEMENT: The downloading and use of this software constitutes acceptance of the following: the software is to be used 'as is' and without modification, you will not distribute the software to other parties (you should direct them to the website, instead), you will not attempt to reverse engineer or extract any part of the software or accompanying data files, and no results beyond reporting the characterization of a single unknown can be published without the express, written consent of the developers.

DISCLAIMER: This software is provided only as an aid to the characterization of skeletal material. The authors accept no responsibility for its ultimate use or misuse. While significant effort has been made to ensure the program is operationally solid and computationally accurate, we provide no warranty and make no specific claims as to its accuracy or its appropriateness for use in a particular situation.

Table of Contents

*** BLANK PAGE ***

INTRODUCTION

The estimation of sex and ancestry are key components when rendering a biological profile from skeletal or other unidentified human remains. The assessment of these traits are critical first steps in a biological profile, as other elements in the analysis of human skeletal remains, such as age and stature, are sex- and ancestry-specific and cannot be adequately determined without this information. The precise estimation of sex and ancestry are also critical in the identification process as they can narrow the search of an unknown individual, which can lead to identification and final disposition of the remains.

Since the 1960's, forensic anthropologists have utilized their knowledge of population variation to develop measurement standards and discriminant functions to estimate sex and ancestry from human remains (Giles, 1964; Giles and Elliot, 1962; Ubelaker et al., 2002). More recently, traditional techniques of size and shape analysis based on linear measurements applied to assembled skeletal data have been used to improve identification methods (Jantz and Moore-Jansen, 1988; Moore-Jansen et al, 1994). Historically, methods of size and shape analysis have relied on the application of multivariate statistical methods (e.g. multivariate analysis of variance, discriminant function analysis, etc.), to sets of caliper measurements that correspond to linear distances, and sometimes to angles (Lynch et al. 1996; Rohlf and Marcus 1993; Ross et al. 1999). One of the major limitations of this type of data acquisition and analysis is that the measurements or angles are ultimately based on the positions of the endpoints, or anatomical landmarks, by which they are defined, yet may encode only incomplete information about the relative positions of these defining points (Bookstein, 1991; Slice, 2005, 2007). In many such cases, for instance, information on biological variation crucial for ancestral determination may not be conveniently oriented along the span of such caliper measurements that are commonly recorded in a traditional analysis (e.g., Ross et al., 1999).

Modern methods of size and shape analysis, called geometric morphometrics (GM), address the potentially serious problems of more traditional approaches by focusing on data and methods that completely and efficiently archive the geometric information recorded from the specimens in a sample (Rohlf and Marcus, 1993; Slice, 2005, 2007). Most often this involves the analysis of the Cartesian coordinates of anatomical landmarks from which any traditional measurement based on the same points can easily be recovered using elementary geometric formulae. Raw Cartesian coordinates, however, are not directly useful as measures of shape (defined as the set of geometric properties of a specimen invariant to size, location, and orientation) or form (defined as shape+size) (Slice et al., 1996). This is because those coordinates are recorded for each specimen with respect to some more-or-less arbitrary set of coordinate axes. As the specimen is moved or rotated, the coordinate values change in complicated ways that are not readily apparent from their numerical values. Since no two specimens can be placed in the same location and orientation with respect to a given set of axes, shape is defined to exclude this potential source of numerical difference and variation in the recorded coordinates. Similarly, the invariance to size accounts for changes in axis scale and sequesters size variation (often dominating statistical analyses) into a separate component. In practice, this situation is dealt with by superimposing and size-standardizing landmark configurations for all specimens onto an iteratively computed mean configurations, a procedure called Generalized Procrustes Analysis (GPA)(see Technical Details). Once so registered, the coordinates for the landmarks of all specimens can be used as shape descriptors for the multivariate analysis of shape (or form) including the discrimination and classification of unknown specimens.

3D-ID is a cross-platform package that allows the forensic practitioner to use these GM methods in the determination of the sex and ancestry of unknown cranial remains. The user provides the program with the Cartesian coordinates of a subset of anatomical points recorded from a cranium of interest. The program then extracts a comparable set of cranial data of known sex and ancestral classification from a reference database of over 1000 individuals. It constructs optimized and landmark-specific classification functions based on this reference subset, and attempts to assign the unknown to one of the available classes for which there are sufficient reference individuals. Diagnostic values are provided in support of this assignment including Mahalanobis squared distance from the unknown to each available reference group mean (upon which the suggested classification is based), sample-adjusted posterior probabilities of membership in all of the available reference groups, and typicality measures for the unknown with respect to each of the available reference groups. The investigator can then use this information, in addition to that from other sources, to inform their professional assessment of the sex and ancestry of the subject material.

The following sections provide step-by-step details of program usage and information on program setup and system requirements. Definitions of landmarks are provided, as are details of the GM and statistical methods implemented in the program.

PROGRAM USAGE

3D-ID is a cross-platform program written in Java. Its use requires a proper installation of Java and the program's own “jar” file. When properly installed, running the program usually involves simply double-clicking the jar file's icon. The Installation, System Requirements, and Troubleshooting section below provides additional, detailed information on initial program setup and problem solving.

The main program window is shown in Figure 1. Because of its cross-platform nature, the program windows may look slightly different depending upon the operating system on which it is being run. Figures in this document show the program running on Mac OS X 10.5.8. Common features include a title bar that can be used to move the window and conrols to minimize, maximize, and exit the program. Below the title bar is the main menu, the details of which will be discussed later. Within the main body of the window is a collection of tabbed panels called “Data”, “Options”, “Report”, and “Log”. Most user interaction takes place through these panels. Their contents are discussed below.

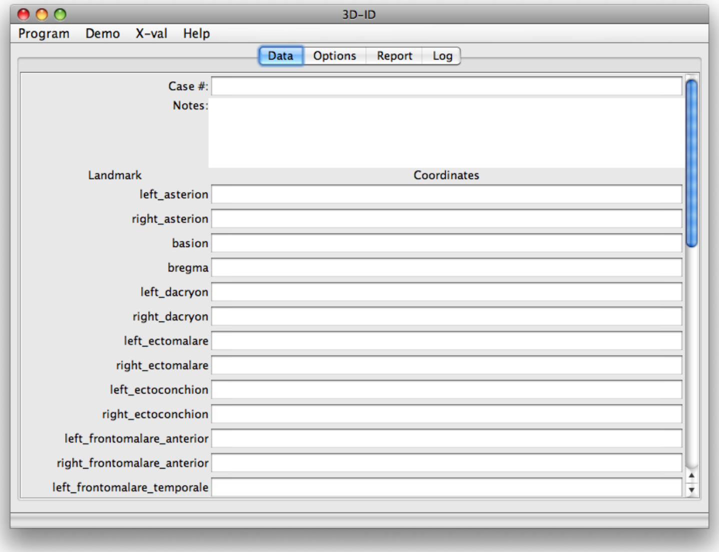

Figure 1: 3D-ID program and data-entry window.

Main Program Panels

The “Data” panel (Figure 1) provides entry areas for a case number and any notes the user would like to include with the analysis. Below this is the main data entry section where the user provides the three-dimensional coordinate values for any of the available 34 landmarks used by the program (see the Landmark Definition section below). The names of the landmarks are listed to the left, and the entry area for the three coordinates for that landmark are to the right. Coordinates are entered as integers or real numbers and separated by spaces (no commas). A scrollbar to the right allows for navigation to hidden areas of the panel. Following the end of the coordinate entry area is a “Process” button that initiates the classification process (Figure 2).

To classify a skull, the investigator minimally provides the raw three-dimensional coordinates for available landmarks on a subject cranium and presses “Process”. Default options are used and the results presented in the “Report” panel with computational details available in the “Log” panel.

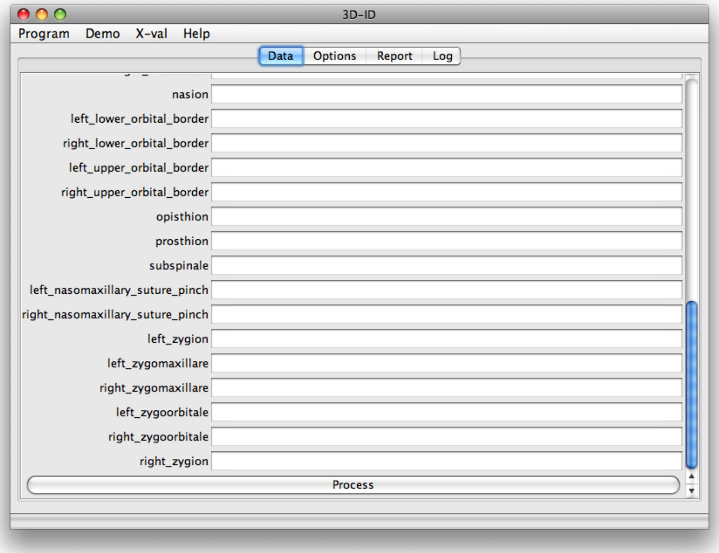

Figure 2: Bottom of data-entry window showing "Process" button.

Options used by the program are presented (and changeable) in the “Options” panel. Clicking on the tab brings up this panel (Figure 3). The uppermost set of user-selectable options deals with details of the classification computations. The first is a check box to direct that size be restored to the coordinates and included in the classification process. The next set of controls allows the user to quickly control which main subsets of potential ancestral groups are to be examined. For the initial choice, “Determine Group and Sex”, both sexes are considered for all ancestral groups. Should ancillary information preclude one sex or the other, the user may elect to compare the unknown only to females or males using one of the next two buttons. For maximum control, every combination of sex and group are listed at the bottom of the panel. The user is free to include (by checking) or exclude (by unchecking) any subset of the groups listed. The actual set of groups to which the unknown is compared, though, is a function of the available reference material and the actual landmarks for which coordinates are available.

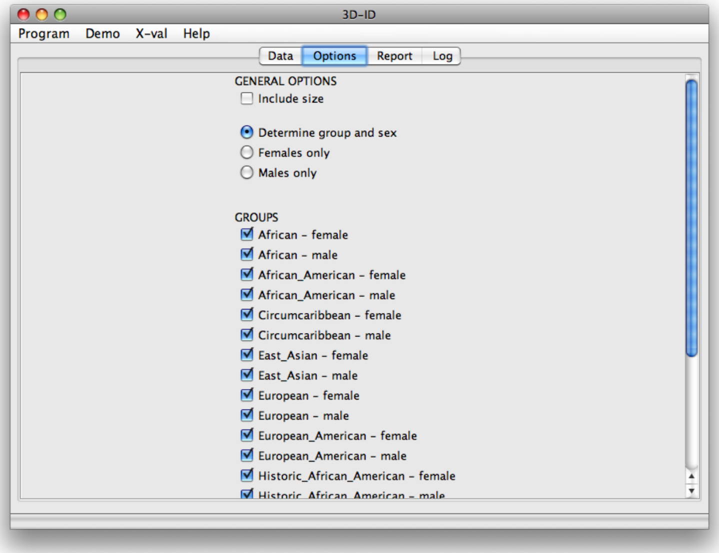

GENERAL OPTIONS

☐ Include size

● Determine group and sex

○ Females only

○ Males only

GROUPS

☑ African - female

☑ African - male

☑ African_American - female

☑ African_American - male

☑ Circumcaribbean - female

☑ Circumcaribbean - male

☑ East_Asian - female

☑ East_Asian - male

☑ European - female

☑ European - male

☑ European_American - female

☑ European_American - male

☑ Historic_African_American - female

☑ Historic_African_American - male

Figure 3: The program "Option" panel.

Pressing the "Process" button on the "Data" panel initiates the classification process. When complete, the results are reported in the "Report" window (Figure 4).

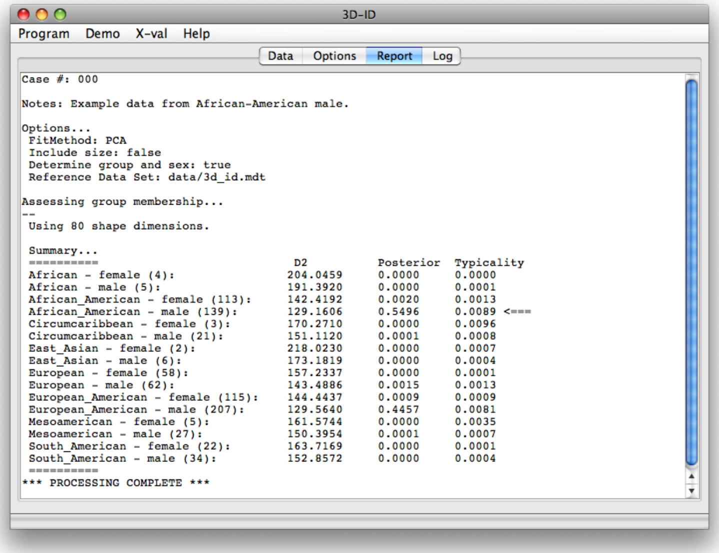

```
Case #: 000

Notes: Example data from African-American male.

Options...
 FitMethod: PCA
 Include size: false
 Determine group and sex: true
 Reference Data Set: data/3d_id.mdt

Assessing group membership...
--
 Using 80 shape dimensions.

 Summary...
 ==========                            D2          Posterior  Typicality
 African - female (4):                204.0459     0.0000     0.0000
 African - male (5):                  191.3920     0.0000     0.0001
 African_American - female (113):     142.4192     0.0020     0.0013
 African_American - male (139):       129.1606     0.5496     0.0089 <===
 Circumcaribbean - female (3):        170.2710     0.0000     0.0096
 Circumcaribbean - male (21):         151.1120     0.0001     0.0008
 East_Asian - female (2):             218.0230     0.0000     0.0007
 East_Asian - male (6):               173.1819     0.0000     0.0004
 European - female (58):              157.2337     0.0000     0.0001
 European - male (62):                143.4886     0.0015     0.0013
 European_American - female (115):    144.4437     0.0009     0.0009
 European_American - male (207):      129.5640     0.4457     0.0081
 Mesoamerican - female (5):           161.5744     0.0000     0.0035
 Mesoamerican - male (27):            150.3954     0.0001     0.0007
 South_American - female (22):        163.7169     0.0000     0.0001
 South_American - male (34):          152.8572     0.0000     0.0004
 ==========
*** PROCESSING COMPLETE ***
```

Figure 4: The program "Report" panel showing classification results.

This particular output is for some data provided with the program for demonstration purposes. The output first shows the case number (if provided by the user) and associated notes. A listing of the parameter values used by the program appears next. The first is the method used in constructing the classification function. This is currently fixed at "PCA" and is described in detail in the "Technical

Details” section. This is followed by the value of the size inclusion parameter, the setting for the group/sex or sex only directive, and the reference database being used in the classification. The latter only changes in the current version of the program for the cross-validation test as explained in the “Main Menu” section. The number of PC axes used, a function of the number of landmarks provided for the unknown and the number of superimposition parameters estimated are shown, and the results of the classification are summarized. The summary includes a list of those reference groups for which there were available data meeting the requirements of the programs parameter values. The number of individuals in each sample is given in parentheses next to the groups label. Next are three columns of numbers including the Mahalanobis squared distance of the (superimposed) unknown to the group mean, the posterior probability of membership in that group as opposed to others that were considered, and the typicality of the unknown specimen should it actually be a member of that group. In the case shown, the unknown was (correctly) assigned to the African-American male reference group consisting of 139 individuals with the same landmarks as the unknown. Its posterior probability of 0.8910 for the chosen group is far higher than that for any other group, and it appears to be a rather typical (p=0.1494) shape for an African-American male – far more so than for other possibilities.

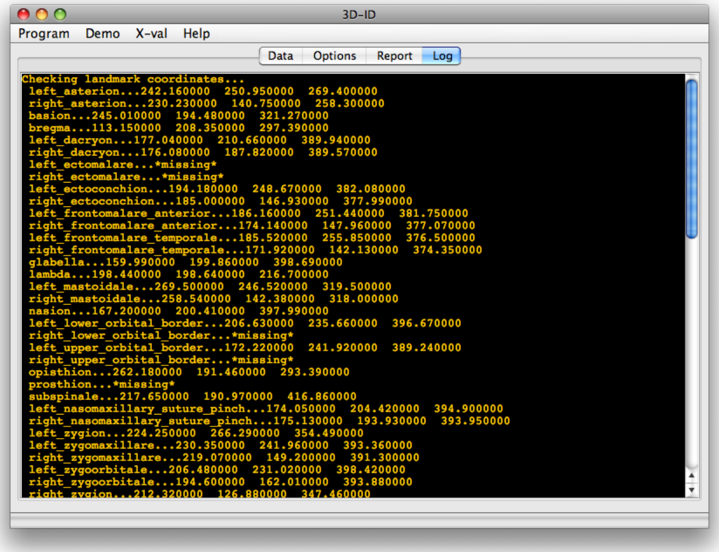

```
Checking landmark coordinates...
 left_asterion...242.160000  250.950000  269.400000
 right_asterion...230.230000  140.750000  258.300000
 basion...245.010000  194.480000  321.270000
 bregma...113.150000  208.350000  297.390000
 left_dacryon...177.040000  210.660000  389.940000
 right_dacryon...176.080000  187.820000  389.570000
 left_ectomalare...*missing*
 right_ectomalare...*missing*
 left_ectoconchion...194.180000  248.670000  382.080000
 right_ectoconchion...185.000000  146.930000  377.990000
 left_frontomalare_anterior...186.160000  251.440000  381.750000
 right_frontomalare_anterior...174.140000  147.960000  377.070000
 left_frontomalare_temporale...185.520000  255.850000  376.500000
 right_frontomalare_temporale...171.920000  142.130000  374.350000
 glabella...159.990000  199.860000  398.690000
 lambda...198.440000  198.640000  216.700000
 left_mastoidale...269.500000  246.520000  319.500000
 right_mastoidale...258.540000  142.380000  318.000000
 nasion...167.200000  200.410000  397.990000
 left_lower_orbital_border...206.630000  235.660000  396.670000
 right_lower_orbital_border...*missing*
 left_upper_orbital_border...172.220000  241.920000  389.240000
 right_upper_orbital_border...*missing*
 opisthion...262.180000  191.460000  293.390000
 prosthion...*missing*
 subspinale...217.650000  190.970000  416.860000
 left_nasomaxillary_suture_pinch...174.050000  204.420000  394.900000
 right_nasomaxillary_suture_pinch...175.130000  193.930000  393.950000
 left_zygion...224.250000  266.290000  354.490000
 left_zygomaxillare...230.350000  241.960000  393.360000
 right_zygomaxillare...219.070000  149.200000  391.300000
 left_zygoorbitale...206.480000  231.020000  398.420000
 right_zygoorbitale...194.600000  162.010000  393.880000
 right_zygion...212.320000  126.880000  347.460000
```

Figure 5: The program "Log" window.

The program “Log” window is for output of technical details that could aid in troubleshooting. The information here provides a more detailed view of the processing than necessary or desirable for the “Report” window. The program first checks each coordinate for each landmark. Each landmark for which data is provided must have three elements that can be translated to decimal values. If no values are provided, the point is marked as “*missing*”. Missing data are acceptable, but data provided for any landmark must be complete. The scroll bar on the right of the window allows the user to scroll down through the listing. The parameters in effect for the classification are listed as in the “Report” window. Information is then provided indicating that the reference database has been opened and the objects matching the groups/sexes selected by the user extracted. These specimens are then filtered to remove any specimen that does not have coordinates for the same landmarks as the unknown. After that, all missing landmarks in the unknown are deleted from the reference samples. Subsequent information shows the progress of the Generalized Procrustes superimposition of the reference samples and the superimposition of the unknown onto the resulting grand mean. At this point, the data have been transformed so that the unknown can be compared to each possible group as described in the "Technical Details" section.

The Main Menu

Most of the program interaction is through the main window panels. However, the main menu provides access to a number of specialized program features and information.

Program: The "Program" menu (Figure 6) provides selections to "Read Data" from a file, "Save Data" to a file, and "Clear Data" from the data panel. Reading and saving data involve a very simple and rigid format. The saved file will have exactly thirty-five lines containing either nothing or the values entered for that landmark in its data entry field. Note that the are only 34 landmarks listed in the data entry field. One has been hidden due to reliability issues, but is still in the reference database and must be accounted for in the data (as missing). So, it must be in the saved data file. A file to be read in must have the exact same format. It is expected that future versions of the program will have a more flexible format for this. Finally, the "Exit" item closes the window and exits the program.

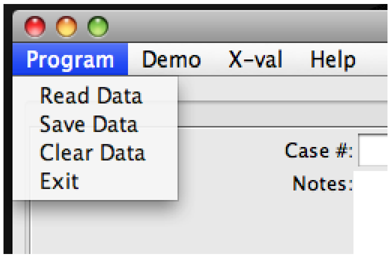

Figure 6: The "Program" menu items.

Demo: The "Demo" menu provides some sample data for easy demonstration of the program. The choices are "African-American Male", "European-American Female", and "European Male" (Figure 7). Selecting any one of these representative configurations will cause the landmark coordinates for the associated specimen to be entered into the landmark coordinate entry fields in the "Data" panel. The user can then click on the "Process" button to see the results of the classification of that individual.

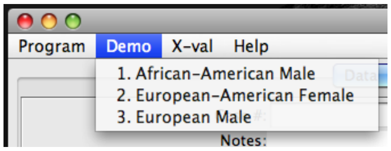

Figure 7: The "Demo" menu items.

X-val: The "X-val" menu provides access to the cross-validation tests used in the development of this program. It was originally included for debugging and testing purposes, but has been made accessible to end users as it provides insight into the operation, capabilities, and accuracy of the program. In the cross-validation process, each specimen is removed from the reference database and treated as the unknown. Classification functions are then constructed based on the remaining specimens and used to classify the excluded individual. In this way, a good estimate of classification accuracy can be obtained since the specimen being classified was not involved in the construction of the classification rule. See “Technical Details” for more information.

The two choices in this menu refer to two databases for which cross-validation can be run. The first is the actual full data set used by the program. This data includes coordinate data for every available landmark for every available skull to maximize the construction of reference samples to which to compare the unknown. Each classification, however, potentially involves different sets of landmarks and different reference subsets making the interpretation of the resulting correct classification rates problematic. Therefore, a second reference database is provided that is a subset of the first containing individuals (over 800) with coordinates for an identical subset of landmarks. This latter reference database is the “Trimmed reference sample”.

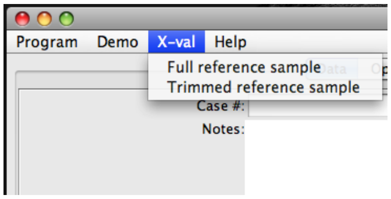

Figure 8: The "X-val" menu items.

Help: The “Help” menu provides access to general information about the program (Figure 9). “About” displays the splash window with authorship and version information. “Credits” list the folks involved in the development of the program and acknowledges the help of those without whose support this project would not have been possible. “Documentation”, for now, simply directs the user to look for this file somewhere. The “Disclaimer” choice brings up our best attempt to let you know the use of this program and/or its output is the sole responsibility of the user and that the authors, while doing their best to provide an accurate and useful piece of software, make no warranties and accept no liability for the accuracy of the information or the appropriateness of the program for a particular purpose. Similarly, the “EULA” item brings up the End User License Agreement that once again puts the burden of responsibility for the use of the program onto the user and prohibits the redistribution or unauthorized use of, or tampering with, the program or its internal data structures. Finally, the “Citation” item presents a suggestion as to how the program should be cited in the literature.

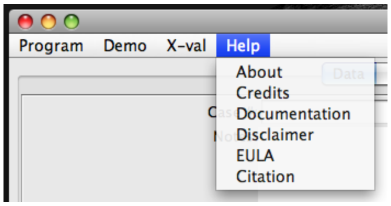

Figure 9: The "Help" menu items.

INSTALLATION AND SYSTEM REQUIREMENTS

System Requirements

- A computer system with an operating system for which the requisite Java environment is available.
- Java 5 (JDK 1.5.x) or higher (http://www.java.com) installed on that system.
- The latest version of 3D-ID available from http://www.3d-id.org

3D-ID is a cross-platform program written in Java. It should run on any system for which an appropriate Java version is available. Mac OS X 10.5, for instance, comes with Java 2 Standard Edition 5.0 (JDK 1.5.x). The latest Java Virtual Machine for all supported operatings systems, e.g., Mac OS X, MS Windows, and Linux, can be downloaded from the Sun site: http://www.java.com Your local computer-support person can help if you have problems.

Basic Installation

If you have an appropriate and functioning Java virtual machine on your computer, installation of 3D-ID is trivial. If you are using a non-Windows system, simply download and save the 3d_id.jar file to an appropriate directory. Windows users need to download and save 3d_id.zip, unzip the file, and move the 3d_id.jar file contained therein to an appropriate directory.

Different downloads are required because MS Windows (Internet Explorer, anyway) automatically changes the ".jar" extension to ".zip", and since MS Windows hides extensions by default, it is unnecessarily complicated to explain to users what is going on and how to fix it.

See your local support person for assistance as needed.

Troubleshooting

If you can run Java programs on a reasonably up-to-date operating system, you should have no problems running 3D-ID. If you do have difficulties, the following can guide your troubleshooting efforts, but it may be a good idea to seek the help of a specialist familiar with your operating system and Java. The information is presented in generic terms. Details may vary slightly depending upon your operating system.

Besides clicking the program icon, you can invoke it from the command line. This affords you the opportunity to see any Java messages should there be a problem. Familiarity with this mode of execution is assumed in subsequent discussions of tracking down Java installation problems. Once all problems are sorted, you can set up an icon with modified parameters to run the program directly from the desktop or other convenient location.

The basic idea is a) open a command-line window, b) change to the directory where the program is stored, and c) have the Java Runtime Environment run the program using:

```
java -jar 3d_id.jar
```

Check to confirm that the program starts and you get no serious error messages. If the program does not run, you should ensure your Java installation is correct by typing, say:

```
java -version
```

The output should look something like this:

```
user:~user$ java -version
java version "1.5.0_20"
Java(TM) 2 Runtime Environment, Standard Edition (build 1.5.0_20-b02-315)
Java HotSpot(TM) Client VM (build 1.5.0_20-141, mixed mode, sharing)
user:~user$
```

The key features here are a) you got actual Java output and b) the version number is greater than 1.5 (=J2SE 5).

3D-ID has a surprisingly small memory footprint, but in some very restricted environments one could run into memory problems. In that case, one run-time parameter you may need to adjust is memory allocation. Maximum memory available to a Java program is set at startup and varies depending upon platform and implementation. You can use the -Xmx parameter to allocated a specific amount of memory that will be available to the program. For development of more memory-intensive programs, I have had good success with 768 megabytes. In this case, the appropriate command line would look like:

```
java -Xmx768M -jar 3d_id.jar
```

You can add this parameter to the command line if you set up a link to the program to run from the Desktop or other location.

LANDMARKS

Initially, up to seventy-five landmarks were collected for each skull depending upon the condition of the skull and the presence of any obvious pathology. A repeatability and digitizing error study carried out as part of this project, however, showed that landmarks defined by remote structures or extremal characteristics, such as euryon, and referred to as Bookstein's Type III landmarks (Bookstein, 1991), were difficult to determine reliably as points for coordinate collection (Ross and Williams, 2008). As a result, thirty-four of the original seventy-five selected landmarks were chosen for use by the program. All are Bookstein Type I (clear juxtapositions of tissues) or Type II (maxima of local curvature, e.g., cusps, invaginations, etc.) landmarks. They are listed and defined in Table 1 and illustrated in Figures 10 to 13 below. Definitions follow Appendix B in Howells (1973) and Moore-Jansen and Jantz (1994). See also http://www.redwoods.edu/Instruct/AGarwin/anth_6_cranial-landmarks.htm. http://www.cleber.com.br/howells.html, http://www.theapricity.com/snpa/gloss2.htm.

Table 1. Thirty-four landmarks used by 3D-ID. Abbreviations used in accompanying figures.		
Landmark	Abbrev	Definition
Left asterion	astl	Intersection of left parietal, left temporal, and occipital bones. If sutures are indistinct or include wormian bones, project suture lines until they intersect.
Right asterion	astr	Intersection of right parietal, right temporal, and occipital bones. If sutures are indistinct or include wormian bones, project suture lines until they intersect.
Basion	bas	The midline point of the anterior foramen magnum margin where it is intersected by the mid-sagittal plane. Directly opposite of the opisthion. In some cases, thickening of the margin can make position location difficult to determine.
Bregma	brg	The midline point where the sagittal and coronal sutures intersect. In cases where the intersection is interrupted, such as with fontanelle bones, the suture lines are projected.
Left Dacryon	dacl	Left eye orbit: point on the medial border where the frontal, lacrimal, and maxilla bones meet, also noted as the intersection of the lacrimo-maxillary suture and frontal bone. A small foramen is often present.
Right Dacryon	dacr	Right eye orbit: point on the medial border where the frontal, lacrimal, and maxilla bones meet, also noted as the intersection of the lacrimo-maxillary suture and frontal bone. A small foramen is often present.
Left Ectomalare	ecml	Left maxilla: positioned at the most lateral point on the lateral surface of the alveolar crest. Found along the second molar on the maxilla.
Right Ectomalare	ecmr	Right maxilla: positioned at the most lateral point on the lateral surface of the alveolar crest. Found along the second molar on the maxilla.
Left Ectoconchion	ectl	Left eye orbit: intersection of the most anterior surface of lateral border and imaginary horizontal line bisecting the orbit.
Right Ectoconchion	ectr	Right eye orbit: intersection of the most anterior surface of lateral border and imaginary horizontal line bisecting the orbit.
Left Frontomalare Anterior	fmal	Left side of skull: most anterior projecting point on the frontomalare suture (different from the frontomalare orbitale and temporale).
Right Frontomalare Anterior	fmar	Right side of the skull: most anterior projecting point on the fronto-malare suture (different from the frontomalare orbitale and temporale).
Left Frontomalare Temporale	fmtl	Left side of the skull: most lateral point on fronto-malare suture
Right Frontomalare Temporale	fmtr	Right side of the skull: most lateral point on fronto-malare suture
Glabella	glb	Most projecting midline point on the frontal bone above

		frontonasal suture. In juveniles with forward vaulted foreheads the most projecting point may not be the glabella.
Lambda	lam	Point where sagittal and lambdoidal sutures meet. If wormian bones are present, project the suture lines to their intersection point.
Left Mastoidale	mastl	Left mastoid process: point is located on the inferior end.
Right Mastoidale	mastr	Right mastoid process: point is located on the inferior end.
Nasion	nas	Midline intersection of the frontonasal suture and mid-sagittal plane.
Left Lower Orbital Border	obhi	Lower border of the left eye orbit: Measured as the maximum height from the upper to the lower orbital borders perpendicular to the horizontal axis of the orbit and using the middle of the inferior border as a fixed point
Right Lower Orbital Border	obhir	Lower border of the right eye orbit: Measured as the maximum height from the upper to the lower orbital borders perpendicular to the horizontal axis of the orbit and using the middle of the inferior border as a fixed point
Left Upper Orbital Border	obhs	Upper left eye orbit: Upper border of the left eye orbit: Measured as the maximum height from the upper to the lower orbital borders perpendicular to the horizontal axis of the orbit and using the middle of the inferior border as a fixed point
Right Upper Orbital Border	obhsr	Upper right eye orbit: Upper border of the left eye orbit: Measured as the maximum height from the upper to the lower orbital borders perpendicular to the horizontal axis of the orbit and using the middle of the inferior border as a fixed point
Opisthion	ops	Midline point of the posterior foramen magnum margin where the mid-sagittal plan intersects. Opposite of basion.
Prosthion-Howells estimated	pr / proHEST	Most anterior, midline point on the alveolar process of the maxilla between the central incisors.
Supspinale	ssp	The deepest point of the profile below the anterior nasal spine.
Left Nasomaxillary Suture Pinch	wnbl-simotic chord	Narrowest portion of the midline of the face to the left naso-maxillary suture. The minimum distance between wnbl-wnbr forms the simotic chord.
Right Nasomaxillary Suture Pinch	wnbr-simotic chord	Narrowest portion of the midline of the face to the right naso-maxillary suture. The minimum distance between wnbl-wnbr forms the simotic chord.
Left Zygion	zygl	Left zygomatic: most lateral point on the zygomatic arch. (Point is determined by measuring bizygomatic breadth)
Left Zygomaxillare	zygoml	Left side of skull: intersection of zygomaxillary suture and most medial masseter muscle attachment.
Right Zygomaxillare	zygomr	Right side of skull: intersection of zygomaxillary suture and most medial masseter muscle attachment.
Left Zygoorbitale	zygool	Left eye orbit: point of intersection between zygomaxillary

		suture and eye orbit.
Right Zygoorbitale	zygoor	Right eye orbit: point of intersection between zygomaxillary suture and orbit border.
Right Zygion	zygr	Right zygomatic: most lateral point on the zygomatic arch. (Point is determined by measuring bizygomatic breadth)

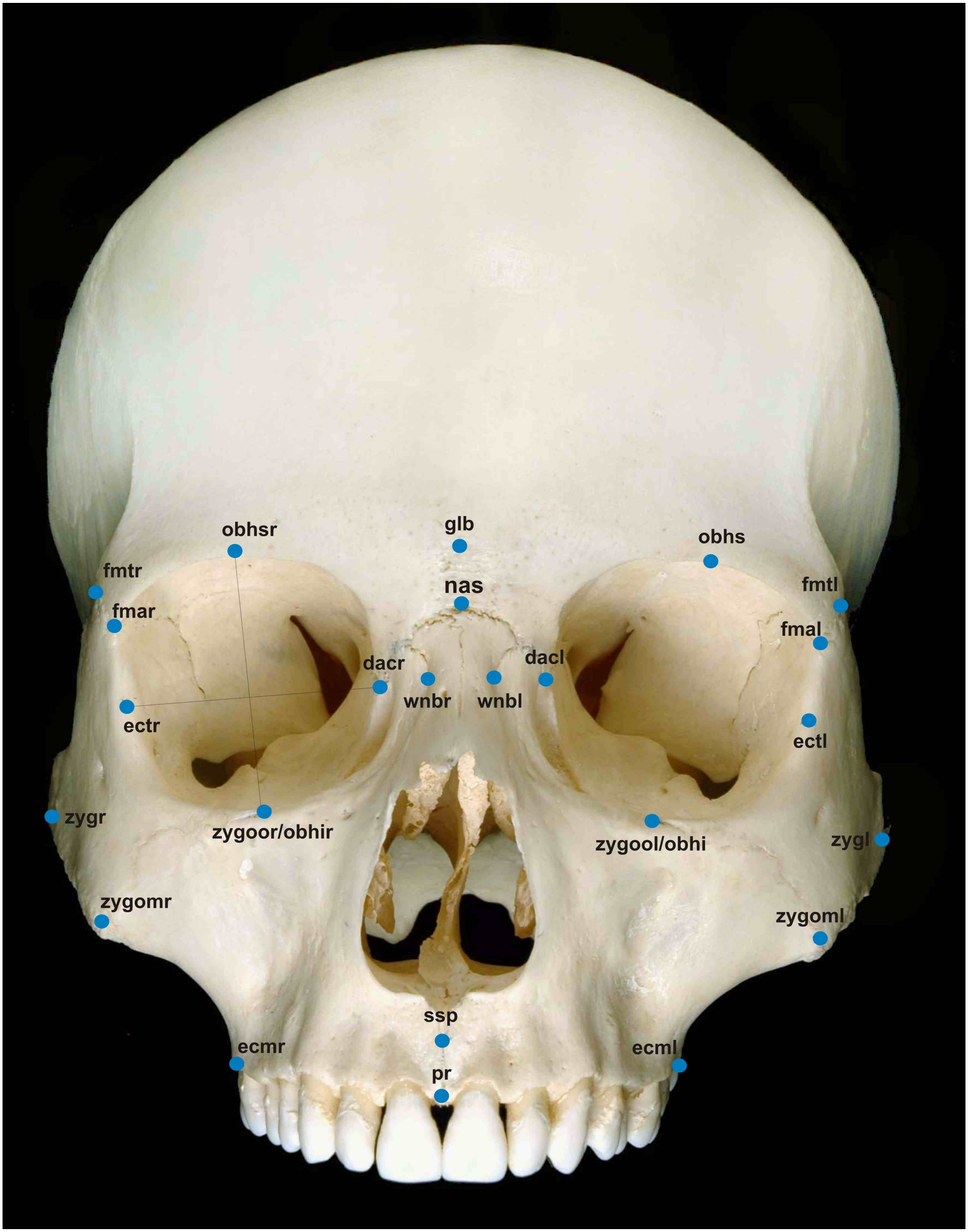

Figure 10: Landmarks used by 3D-ID: anterior view.

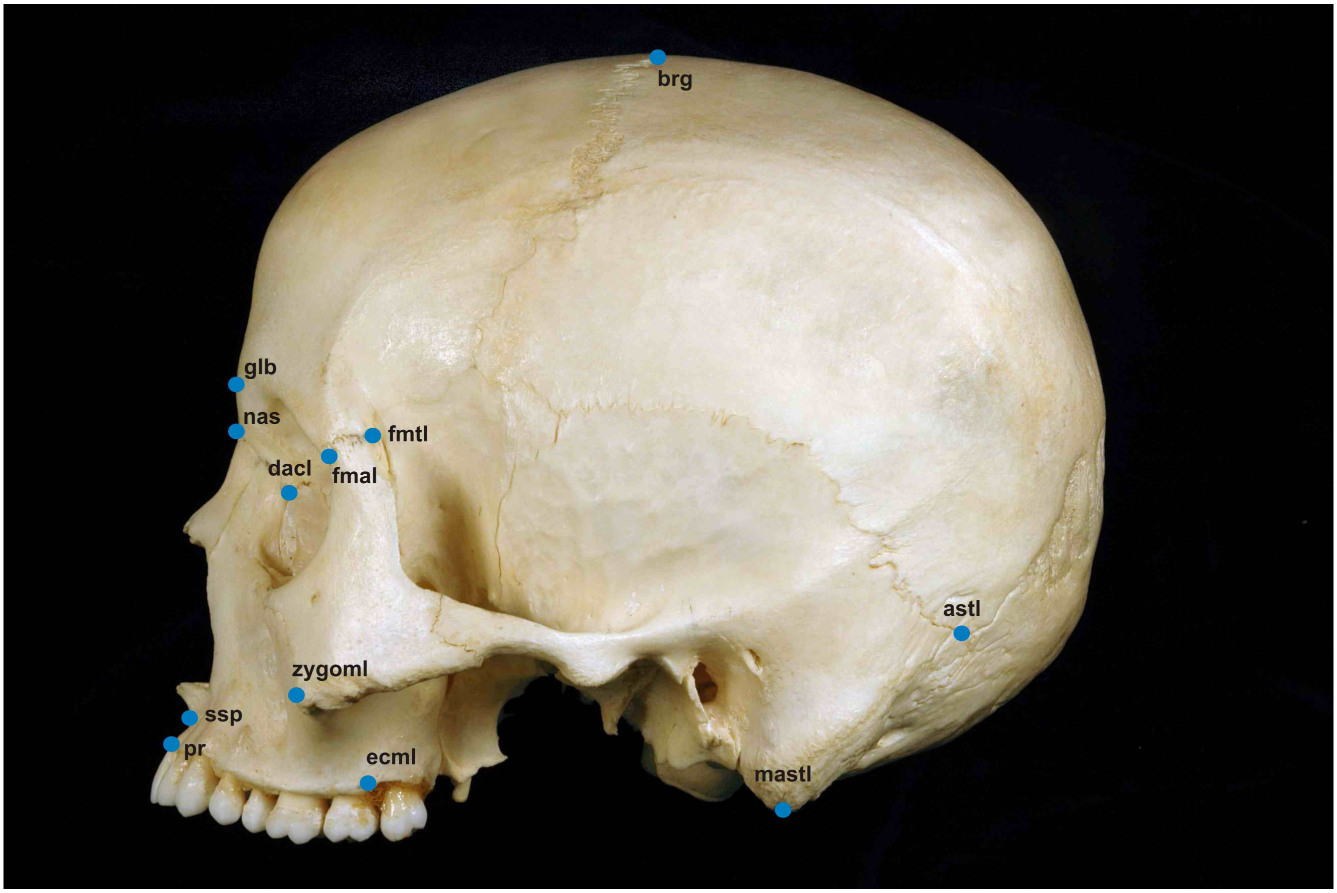

Figure 11: Landmarks used by 3D-ID: lateral view.

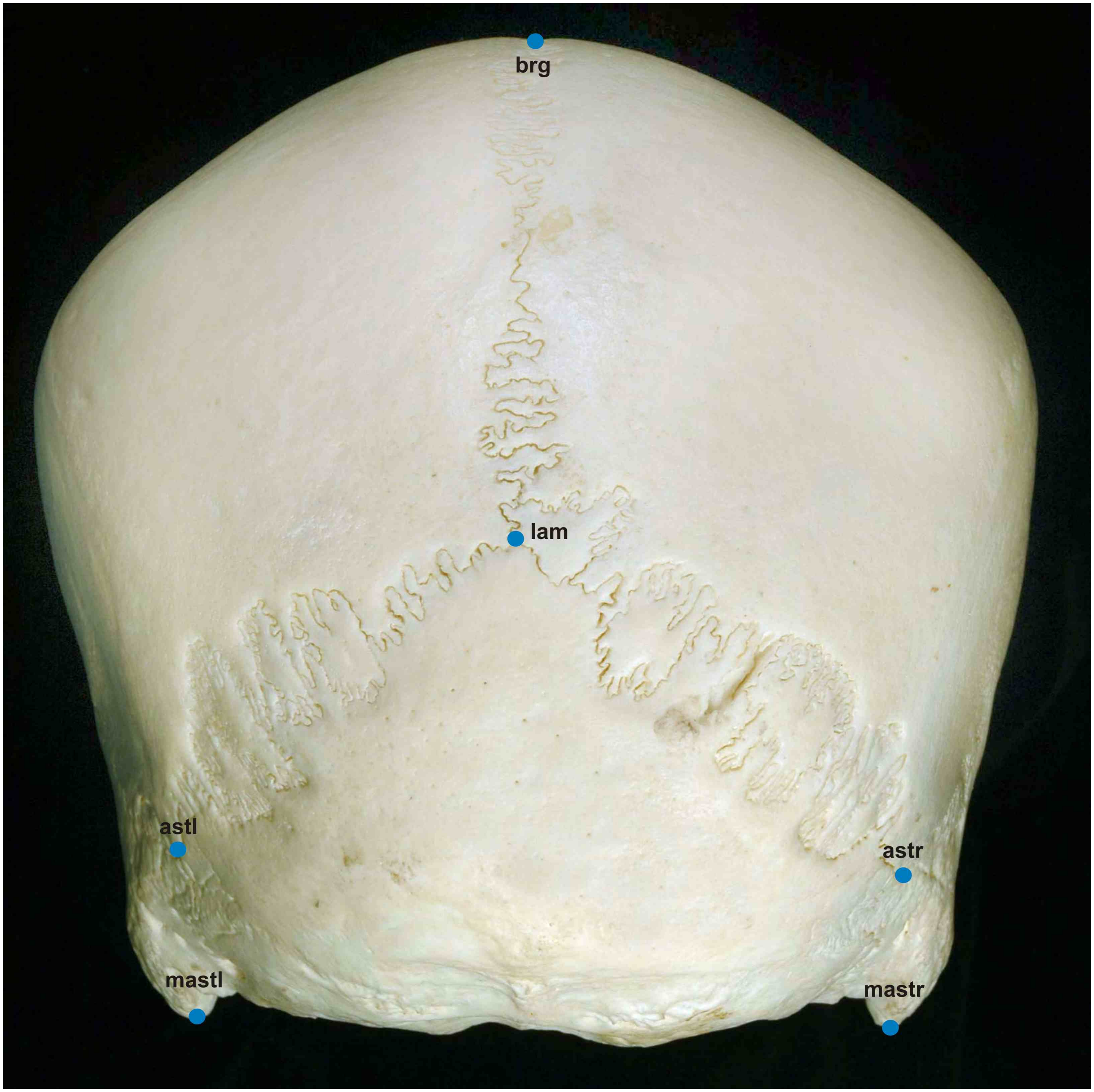

Figure 12: Landmarks used by 3D-ID: posterior view.

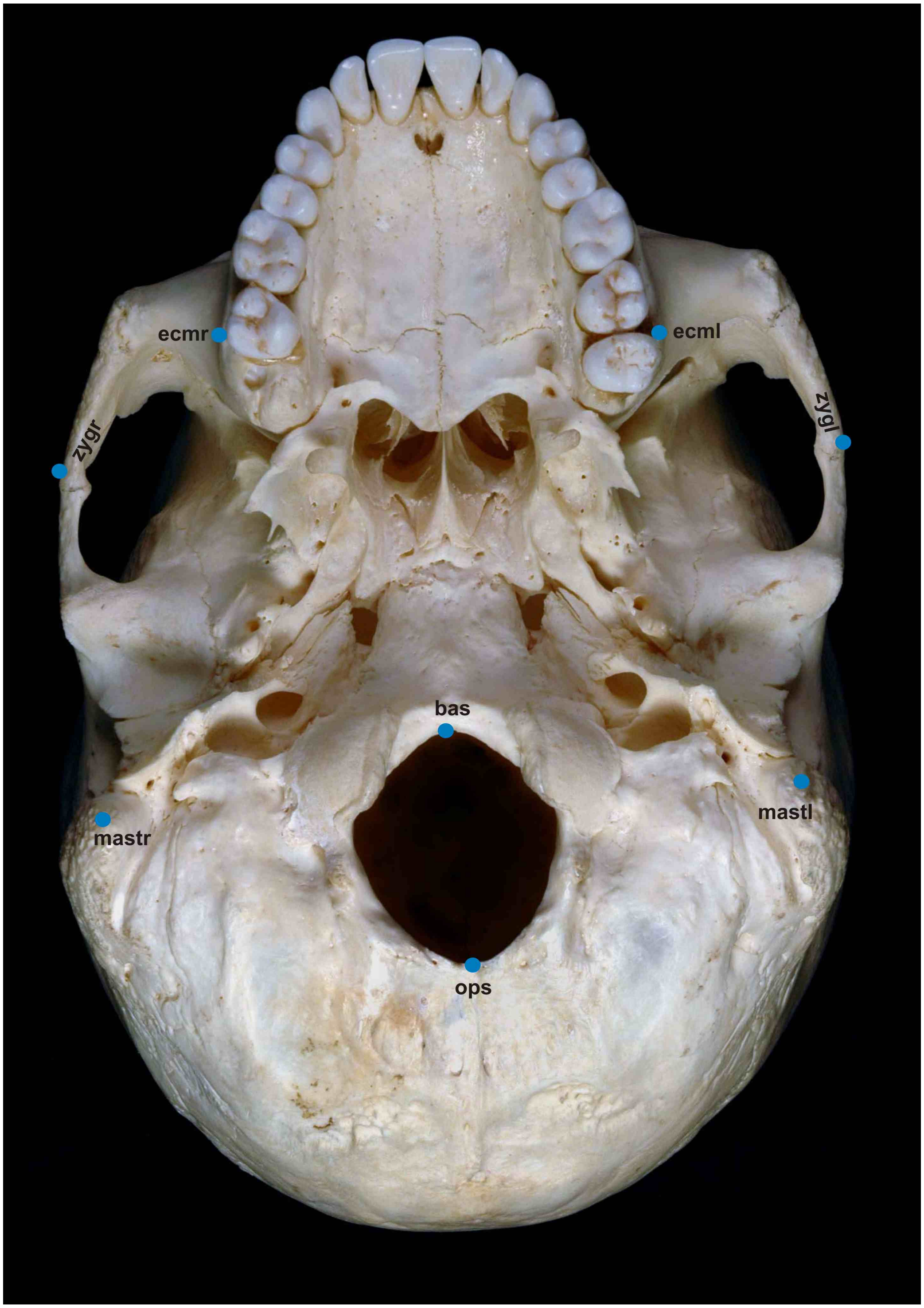

Figure 13: Landmarks used by 3D-ID:inferior view.

REFERENCE DATA

Reference data were collected from skeletal remains with known demographics (e.g. ancestry, age, and sex) from national and international forensic laboratories and museums. In addition, we re-evaluated currently used ancestral classifications to improve correct allocations of unknown individuals. As such, present day classifications systems do not necessarily have biological meaning. For example, the term "Hispanic" includes all Spanish speaking peoples and does not adequately address the distinct ethnohistorical origins of the populations – it is a biologically meaningless term (Ross et al. 2004). To address these shortcomings, we divided our reference populations into geographic regions represented by closely related populations (e.g. Mesoamerican, Circumcaribbean, South American, European American, European, etc.). Although there is still much variation within each region, these groupings better address the biological similarities and differences among these closely related populations. In addition, as European Americans are an amalgamation of numerous European groups, we did not group them together with individuals from Europe. The same holds true for individuals of African origin. It will be an ongoing process to locate underrepresented groups such as Asians, Central Americans, Puerto Ricans, etc., which will be included in the database as they become available.

The current reference collection includes 1089 individuals, which will increase as newly acquired samples are included (see Table 2). Only trauma- and pathology-free individuals were included in the reference population. The reference sample was amassed from various national and international museum collections and laboratories and from many researchers kind enough to provide their data for this endeavor. Museum collections included in this project are: Maxwell Museum in Albuquerque, New Mexico, USA; Samuel Morton Collection at the Penn Museum, University of Pennsylvania (http://penn.museum/documents/publications/expedition/PDFs/50-3/renschler.pdf), Philadelphia, Pennsylvania, USA; American Museum of Natural History, New York, New York, USA; Luis Lopes Collection at the Bocage Museum in Lisbon, Portugal; Oloriz Collection in Spain (http://www.ucm.es/info/museoana/Colecciones/Craneos/index_english.htm); Juan Munizaga Collection curated at the Universidad de Chile, Santiago, Chile; The Donated Collection at the University of Tennessee, Knoxville, Tennessee, USA; C.A. Pound Human Identification Laboratory at the University of Florida, Gainesville, Florida, USA; Morgue Judicial, Republic of Panama; North Carolina Office of the Chief Medical Examiner, USA; and the Georgia Bureau of Investigation, USA.

Sex (male or female) is used to further subdivide the reference data. Some individuals in the reference database may be excluded from any consideration due to a lack of critical assignment information. For instance, sex is unknown for some individuals, and neither group nor sex is known for three. These specimens were, however, retained in the reference data set for completeness and possible future use.

Table 2. Sample Composition. Total sample N = 1089.

	Female	Male	Unknown
African	5	6	16
African American	123	149	0
Circumcaribbean	4	22	0
East Asian	2	9	0
European	59	71	90
European American	134	238	0
Historic African American	1	0	0
Mesoamerican	8	35	1
South American	35	44	3
Unknown	3	18	10

TECHNICAL DETAILS

Shape is defined as the geometric properties of an object that are invariant to location, orientation, and scale (=size), and *form* is defined as shape + size (Slice et al. 1996). Specifying an invariance to location and orientation seems straightforward as one generally does not want the measurements under consideration to vary with where the object is measured or how it is rotated. Size, on the other hand, often tends to dominate variation in biological samples and may or may not contribute meaningful signal in doing so. Therefore, morphometrics analysis focuses on the isolation of shape variation as per the above definition while factoring out and sequestering a size component that may or may not be considered alone or with shape (form) depending upon the investigators goals and insight.

Traditional (curvi-)linear distances and angular measurements vary in their appropriateness as shape variables. Distances between points on an object are, in fact, invariant to the location and orientation of the object from which they are obtained, but they carry with them size information. This can be partially remedied by the construction of “indices” that are of the form, I = 100 * (d1/d2). This records one measured distance relative to another on the same specimen and removes size from between-specimen comparisons. Angles are invariant to location, orientation, and size, and are, thus, proper shape variables.

Figure 14 illustrates part of the problem with traditional measurements in morphometric analysis. The size dependence of the distances between nasion (n) and basion (ba) and the distance from basion to prosthion (pr) can be addressed by the construction of the gnathic index, $I_g = 100 \times (d(n\text{-}ba)/d(ba\text{-}pr))$. This, however, introduces the complex characteristics of ratios into the problem and still fails to fix the relationship between nasion and prosthion. Adding the angle between the two segments addresses that problem, but mixes units in the data. Adding a second second index, $I_{g(n\text{-}pr)} = 100 \times (d(n\text{-}pr)/d(ba\text{-}pr))$ works, too, but as more and more points are considered the requisite number of carefully chosen distances needed to capture all of the geometry rapidly proliferates. The example is two-dimensional, but these considerations apply with even greater force in three.

One approach to the above problem taken by GM is to focus on the analysis of the coordinates of anatomical points instead of the distances between them or the angles they form (Figure 15). Coordinates, though, vary as a function of the location of an individual specimen with respect to more-or-less arbitrary digitizing axes used for data collection. This requires some pre-processing of the data to construct proper shape variables, but they retain all geometric information that could be collected from distances and angles defined by the same points. That pre-processing step usually involves the registration of the configurations of landmarks for all specimens into a common coordinate system using a least-squares estimation of location and orientation parameters and a reasonable size standardization. This approach, in which data from individual specimens are fit to an iteratively computed mean configuration, is called Generalized Procrustes Analysis (GPA) (Gower, 1975; Rohlf and Slice, 1990). After superimposition, the landmarks can be subjected to familiar multivariate procedures including discrimination and classification methods. Since all intrinsic geometric information is retained, graphical reconstructions in physical space of many multivariate statistical results are possible, though these are less useful in the current application.

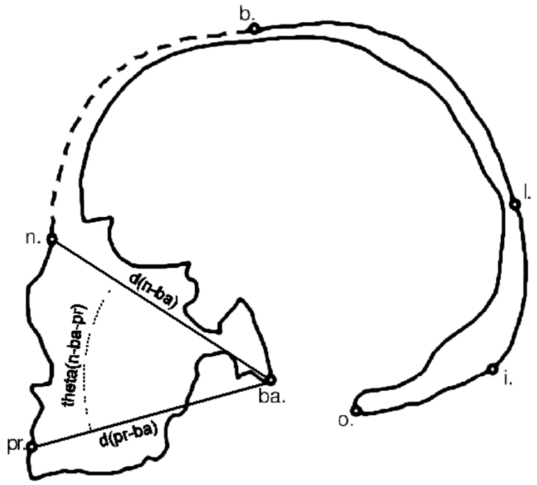

Figure 14: Traditional measurements based on anatomical landmarks. Landmarks are prosthion (pr), nasion (n), bregma (b), lambda (l), inion (i), opisthion (o), and basion (ba). Measurements are the distances between nasion and basion , d(n-ba), and between prosthion and basion, d(pr-ba). Theta(n-ba-pr) is the angle formed at basion by the three points. See text for details.

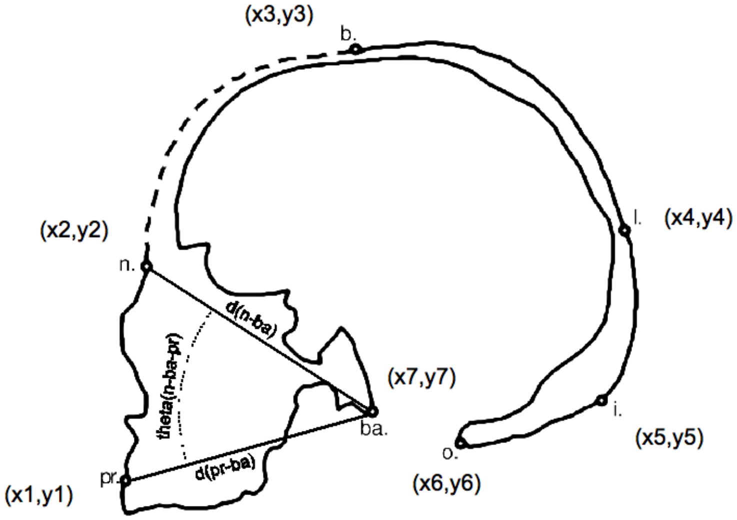

Figure 15: Anatomical landmark positions encoded as Cartesian coordinates.

3D-ID implements this approach to help characterize unknown human remains (specifically, cranial remains at this time). To do this, the user provides the program with three-dimensional coordinates of a subset of the landmarks described above. A reference database is then processed to extract appropriate reference samples. Then, the unknown is compared to the groups available in the reference sample to estimate group membership. Separate groupings are considered for each sex, but if sex can be determined by other means, the comparisons can be easily restricted to only female or male groups. The details of how this is accomplished follow:

Initial Data Checking and Filtering: When the "Process" button is clicked, 3D-ID examines the entry for each listed anatomical point (landmark). It checks to make sure there are three numerically valid values for any landmarks for which data are provided. If no data are provided, it is assumed that landmark is missing or excluded from the unknown. Once the program determines that there exists an error-free subset of landmarks available for analysis, it turns its attention to the reference database. The reference database (currently containing over 1000 specimens) is scanned and any object that does not contain at least the landmarks specified for the reference is deleted. This results in an unknown with some number of valid 3D coordinates for some number of landmarks and the remainder marked as missing and a reference database within which all objects have coordinates for the non-missing ones provided for the reference.

All landmarks marked as missing in the unknown are then deleted from the data structure for the unknown and from all remaining reference specimens. The result is an unknown with 3D coordinates provided from some subset of landmarks and a reference set consisting of all members of the original reference database edited so as to have the same landmarks as the unknown. At this point, all objects, whether unknown or reference, have the same number of landmarks and no missing data.

Procrustes Analysis: The entirety of the reference data are then subjected to a Generalized Procrustes Analysis. This is an iterative procedure that translates and rotates landmark configurations to minimize the sum of squared deviations of individual landmarks to their homologues on an iteratively computed mean, or reference, configuration. Prior to iterating, the optimal translation is obtained once and for all by mean-centering every individual configuration of landmarks – the sum of coordinate values for any one configuration equals zero. The iteration begins by the selection of any configuration of landmarks (in this case the first in the reference sample) as an estimate of the mean, fitting the data to that, recomputing the mean, and repeating until convergence. Optimal rotation at each of these steps is achieved by multiplying the mean-centered configuration, $\mathbf{X}_i$, where $\mathbf{X}_i$ is a p landmarks by k dimension matrix for the ith configuration, by:

$$\mathbf{H}_i = \mathbf{V}_i \mathbf{S}_i \mathbf{U}_i^{\mathrm{t}}$$

Here, $\mathbf{V}_i$ and $\mathbf{U}_i$ are orthonormal rotation matrices computed by singular value decomposition as:

$$\mathbf{X}_{\mathrm{ref}}^{\mathrm{t}} \mathbf{X}_i = \mathbf{U}_i \Sigma_i \mathbf{V}_i^{\mathrm{t}}$$

The matrix $\mathbf{X}_{\mathrm{ref}}$ is the current estimate of the reference configuration. The matrix $\mathbf{S}_i$ is a diagonal matrix of ones with the same sign as the corresponding diagonal elements of $\boldsymbol{\Sigma}_i$ and ensures the rotation is rigid and does not stretch the configuration to achieve a reduction in the sum of squares (using $\boldsymbol{\Sigma}_i$ would do that).

Scaling occurs once and for all along with the translation prior to iteration, but it is not least-squares based. Instead, configurations are scaled so that the square root of the sum of squared deviations of all the points from their centroid is 1.0. This measure, called Centroid Size (CS), has certain logical and optimal properties that recommend it here (see Bookstein, 1991), and its use results in all specimens being scaled to the same (CS=1.0) size, thus removing size variability (as defined by CS) from the reference data.

Further details and discussion of these procedures can be found in Slice (2005, 2007) that provide appropriate and more extensive citations.

Dimensionality considerations: The variables capturing the shape of the unknown are three-dimensional point coordinates. Their analysis, however, involves a much higher dimensional space – at most, the number of coordinate dimensions, 3, times the number of points (variable). The actual variability realized in the space may, in fact, be of lower dimensionality. Such a case leads to data covariance matrices with zero eigenvectors that can cause problems with multivariate operations involving the inverse of the covariance matrix (a division by zero situation). The Procrustes superimposition, itself, guarantees a loss of variability. For 3D data after GPA, six directions in multivariate space are associated with precisely zero variability and a seventh with near-zero variability, near zero due to a slight curvature of the variation introduced by the superimposition (Slice, 2001).

3D-ID address these issues at several levels. First, it calculates the maximum possible dimensionality of the variation possible with the number of points specified for the unknown. It then adjusts this value for those lost due to superimposition. Further, the program uses algorithms robust to the presence of zero eigenvalues and excludes those with empircally near-zero values for the relevant data set.

The details of how and when these controls come into play are described as they arise in the classification process.

It is worth noting that it is a common practice when using standard software packages to address this issue by subjecting a few principal components with substantial variation to routines that could not otherwise handle the case of zero eigenvectors. Once a reduced number of data PCs have been selected for analysis, though, any subsequent *p*-values, e.g., tests of group differences on one or more PCs, are suspect. The PCs extract combinations of the variables with greatest variance, and this may or may not be driven by the differences inspected by statistical tests. A usual case is to deflate the *p*-values (making them look more significant) when group differences contribute a great deal to the sample variation. This is not a major issue for 3D-ID as the focus is maximizing correct classifications and not estimating actual probabilities.

Discriminant Analysis: The classification routine implemented in the current version of the program involves assignment of the unknown to the group from whose mean it has the smallest Mahalanobis squared distance. This distance is computed as:

$$D_i^2 = \left(\boldsymbol{x}_{\text{unknown}} - \bar{\boldsymbol{x}}_i\right)^{\text{t}} \mathbf{S}_{\text{pooled}}^{-1} \left(\boldsymbol{x}_{\text{unknown}} - \bar{\boldsymbol{x}}_i\right)$$

The D_i^2 is the squared Mahalanobis distance of the unknown to the *i*th group mean. The $\mathbf{S}_{\text{pooled}}^{-1}$ is the pooled, within covariance matrix for the data in the space of the sample PCs excluding those expected to have zero, or near-zero, eigenvectors (seven for 3D coordinates). To guard against additional problems caused by singularities in $\mathbf{S}_{\text{pooled}}$ due to actual restricted variation in the reference data or sample size limitations, 3D-ID uses, instead of the standard matrix inverse, the Moore-Penrose inverse, $\mathbf{S}_{\text{pooled}}^{+}$, computed from the singular-value decomposition of $\mathbf{S}_{\text{pooled}}$. The program excludes components with near-zero (10^-12) variances that can destabilize the matrix inversion.

Note that the configurations, **x**s, are now vectors (instead of matrices with rows representing points and columns their coordinates). Once the GPA process is completed, the data are converted to vectors initially with dimension nLandmarks × nDimensions. The reference data are then organized into a matrix with rows for every specimen and columns for every dimension for every landmark.

As implemented, the reference data are projected into the reduced space of the PCs excluding those with expected (near-)zero variation. This is done by multiplying the (mean-centered) data matrix on the right by the first (nPointsInTheUnknown × 3 - 7) eigenvectors of **S**, the superimposed reference sample total covariance matrix. After this, the pooled, within group covariance matrix is computed by pooling the deviations of members of all groups from their own group mean. This matrix, $\mathbf{S}_{\text{pooled}}$, forms the basis for the computation of the Mahalanobis squared distances described above, though the exact computation is a little different.

The above formula shows how to transform the distance between a specimen (the unknown) and a group mean into a Mahalanobis squared distance by use of the inverse, pooled covariance matrix. The same result can be obtained by transforming the space of all specimens by this matrix and, then, computing Euclidean distances in that space. This is what is done in 3D-ID. First, the unknown is fit to the grand reference mean using an Ordinary Procrustes Analysis (a non-iterative implementation of the above that fits one configuration to another, specific configuration instead of an iteratively computed mean). Then, the fitted unknown is projected into the reduced space of the reference sample using the same eigenvectors that were used for the reference data. This transformed unknown and all of the group means in this reduced space are then mapped into a transformed space by multiplication by $\mathbf{S}^{+}_{\text{pooled}}$. Squared, Euclidean distances between the unknown and each group mean are then computed, and these are the familiar Mahalanobis squared distances.

The Mahalanobis squared distances are standardized distances accounting for the covariance structure of the data, but may not look familiar as standard deviations. This is because these are distances in a multidimensional space where each dimension can add to the value of the distance. Additional steps must be taken to convert them into a probability of group membership (even in light of the warning about using PCs for such probabilities as previously mentioned).

Assignment of the Unknown: The suggested assignment of the unknown is to that of the available groups for which the unknown has the smallest D_i^2. This is not necessarily as clear cut a statement as one might hope, so several other diagnostic measures, assuming multivariate normal distributions, are provided to aid in the evaluation of the suggested assignment following Campbell (1984).

The suggested assignment is based on the lowest D_i^2, but the distances to other groups might be fairly similar. To help gauge the strength of the suggestion in this regard, a "posterior probability" is provided for each group. This measures the relative closeness of the unknown to each group. In the most clear cut case, there will be one very high value associated with the suggested assignment with values for the other groups near zero. In a more ambiguous case, one or more groups may have lower, but similar, posterior probabilities to that of the suggested assignment. This indicates that while the unknown was slightly more similar to the recommended group, it was nearly as similar to one or more other groups. In such cases, the recommended assignment should be viewed with caution.

The proper computation of the poster probabilities for multivariate data should take unequal sample sizes and estimated parameters into account. Assuming equal prior probabilities of being in any of the reference groups, the posterior probability of membership in the *i*th group is:

$$\Pr\left(\boldsymbol{x}_{\text{unknown}}\right)_i = \frac{\mathrm{f}\left(\boldsymbol{x}_{\text{unknown}}\right)_i}{\sum_{j=1}^{g} \mathrm{f}\left(\boldsymbol{x}_{\text{unknown}}\right)_j}$$

Here, f() is the probability density function for the unknown and the group specified in the subscript. With unequal sample sizes and estimated means and covariance structures, this the leads to:

$$\mathrm{f}\left(\boldsymbol{x}_{\text{unknown}}\right)_i = \pi^{-v/2} \frac{\Gamma\left((n_f+1)/2\right)}{\Gamma\left((n_f-v+1)/2\right)} \left| \frac{(n_i+1)\,n_f}{n_i} \boldsymbol{S}_{\text{pooled}} \right|^{-1/2} \left(1+\frac{n_i D_i^2}{n_f(n_i+1)}\right)^{-(n_f+1)/2}$$

In this equation, v is the dimensionality of the space of the reference data (probably reduced by PCA), n_i is the size of the ith reference group, $n_f = \sum_{i=1}^{g} \left(n_i - 1\right)$, and Γ() is the gamma function. Again, the generalized inverse is used by the program to address singularities and avoid instabilities.

The second diagnostic measure provided by the program is a “typicality” measure. This is simply the probability of an observation being as far or farther away from the mean as the unknown for a particular group. Typicality measures how likely it is that the unknown came from a particular population at all. For instance, an unknown will *always* be suggested as belonging to one of the available reference groups, but typicality measures how likely that is to be true for any given population. That is, the unknown could be suggested for membership in one (the closest) population, but still be so different that the probability of actually finding a specimen that different from the population is small. Again in such cases, the suggested assignment should be taken with an appropriate degree of skepticism. Typicality is computed by finding the probability of:

$$\frac{\left(n_f - v + 1\right) n_i}{v\, n_f \left(n_i + 1\right)} D_i^2$$

for an F distribution with v and $n_f - v + 1$ degrees of freedom, $\mathrm{F}(v, n_f - v + 1)$.

In general, then, the program will suggest an assignment to the group whose mean is closest in the Mahalanobis sense to the unknown. Posterior probabilities can be used to assess how strong the evidence is this assignment versus that for assignment to other reference groups. The typicality can be used to assess how likely the unknown is to have come from a particular population regardless of how much closer it is to it than the other populations or how much that difference is similar to other such differences.

REFERENCES

Bookstein, F. L. 1991. *Morphometric tools for landmark data: geometry and biology*. Cambridge Univ Press.

Campbell, N. A. 1984. Some aspects of allocation and discrimination. In *Multivariate Statistical Methods in Physical Anthropology* (G. N. van Vark and W. W. Howells, eds.), 177-192. D. Reidel Publishing.

Giles, E. 1964. Sex Determination by Discriminant Function Analysis of the Mandible. *American Journal of Physical Anthropology* 22: 129-135.

Giles, E. and O. Elliot. 1962. Race Identification from Cranial Measurements. *Journal of Forensic Sciences* 7: 147-157.

Gower, J. C. 1975. Generalized Procrustes analysis. *Psychometrika* 40(1): 33-51.

Howells, W. W. 1973. Cranial variation in man; a study by multivariate analysis of patterns of difference among recent human populations. Papers of the Peabody Museum of Archaeology and Ethnology Harvard University, Cambridge, Massachusetts, USA. Volume 67.

Jantz, R. L., and P. H. Moore-Jansen. 1988. *A Data Base for Forensic Anthropology: Structure, Content and Analysis*. Report of Investigations No. 47. Department of Anthropology, The University of Tennessee.

Lynch, J. M., C. G. Wood, and S. A. Luboga. 1996. Geometric morphometrics in primatology: Craniofacial variation in Homo sapiens and Pan troglodytes. *Folia Primatologica* 67(1): 15-39.

Moore-Jansen, P. and R. Jantz. 1994. Data collection procedures for forensic skeletal remains. Report of investigations / University of Tennessee, Dept. of Anthropology ; -- no. 48

Moore-Jansen, P. H., S. D. Ousley, and R. L. Jantz. 1994. *Data Collection Procedures for Forensic Skeletal Material*. 3rd ed. University of Tennessee Forensic Anthropology Series. Knoxville, Tenneessee.

Rohlf, F. J. and L. F. Marcus. 1993. A Revolution in Morphometrics. *Trends in Ecology and Evolution* 8(4): 129-132.

Rohlf, F. J. and D. E. Slice. 1990. Extensions of the Procrustes method for the optimal superimposition of landmarks. *Systematic Zoology* 39(1): 40-59.

Ross, A. H., A. H. McKeown, and L. W. Konigsberg. 1999. Allocation of crania to groups via the "new morphometry". *Journal of Forensic Sciences* 44(3): 584-587.

Ross A. H., D. E. Slice, D. H. Ubelaker, and A. B. Falsetti. 2004. Population Affinities of 19th Century Cuban Crania: Implications for Identification Criteria in South Florida Cuban Americans, *J Forensic Sci* 49:11-16.

Ross A. H., S. E. Williams. 2008. Testing Repeatability and Error of Coordinate Landmark Data Acquired from Crania. *Journal of Forensic Sciences* 53: 782-5.

Slice, D. E. 2005. *Modern Morphometrics in Physical Anthropology*. Springer.

Slice, D. E. 2007. Geometric morphometrics. *Annual Review of Anthropology* 36: 261-281.

Slice, D. E., F. L. Bookstein, L. F. Marcus, and F. J. Rohlf. 1996. A glossary of geometric morphometrics. In *Advances in Morphometrics*, 284:531-551. NATO ASI Series Series A: Life Sciences. New York: Plenum Press.

Ubelaker, D., A. Ross, and S. M. Graver. 2002. Application of Forensic Discriminant Functions to a Spanish Cranial Sample. *Forensic Science Communications* 4, no. 3. http://www.fbi.gov/hq/lab/fsc/backissu/july2002/ubelaker1.htm.

*** NOTES ***